Energy transfer processes in holmium and erbium doped silicon

J. F. Suyver

Supervisors:
- Drs. P. G. Kik
- Prof. Dr. A. Polman

FOM Institute for Atomic and Molecular Physics
Kruislaan 407, 1098 SJ Amsterdam
The Netherlands

Verslag van het groot onderzoek voor de afstudeerrichting Experimentele Natuurkunde aan de faculteit Natuur- en Sterrenkunde van de Universiteit Utrecht.

13 oktober 1997 – 1 februari 1999

Table of Contents

	Table of Contents	page 3
	Introduction and acknowledgements (Dutch)	page 5
1.	Optical and electrical doping of silicon with holmium	page 7
2.	Holmium in amorphous Si:O, N, H	page 13
3.	Energy transfer in Si:Er *p-n* diodes	page 15
A.	Abstract for the NEVAC studentendag conference, April 3 1998, Venlo	page 23
B.1.	Abstract for the 11th International Conference on Ion Beam Modification of Materials, August 31 – September 4, 1998, Amsterdam, The Netherlands	page 25
B. 2.	Poster for the IBMM98 conference	page 27

The work presented in this Master's thesis was published in

- J. F. Suyver, P. G. Kik, T. Kimura and A. Polman, G. Franzò and S. Coffa, Nucl. Instr. and Meth. in Phys. Res. B **148**, 497 (1999).
- N. Hamelin, J. F. Suyver, P. G. Kik, K. Kikoin and A. Polman, A. Schönecker and F. W. Saris, M. A. Green, to be published.

And was presented at the following conferences

- NEVAC (Dutch Vacuum Society) Studentendag, April 3, 1997, Océ Technologies, Venlo. The Netherlands.
- 11th International Conference on Ion Beam Modification of Materials, August 31 – September 4, 1998, Amsterdam, The Netherlands.

Voor iedereen!

In het derde en vierde jaar van de studie natuurkunde in Utrecht, volgt de student een aantal keuzevakken. Een van de vakken die ik toen gevolgd heb was "Materiaalonderzoek op atomaire schaal" van Prof. Albert Polman. Een onderdeel van dit college was een excursie naar het FOM-instituut voor atoom- en molecuulfysica in Amsterdam, de thuisbasis van Alberts onderzoeksgroep.

Na deze kennismaking met het amolf, heb ik een jaar later besloten om mijn afstudeeronderzoek op het amolf te doen en wel in de groep van Albert. Deze groep (opto-electronic materials) doet onderzoek aan de optische eigenschappen van nieuwe materialen. Deze materialen worden dan vaak eerst zelf gemaakt voordat er metingen aan gedaan kunnen worden.

Het onderzoek dat ik heb gedaan ging vooral over luminescentie. Dit is de eigenschap van materialen om licht uit te zenden van een andere kleur dan het (groene) laser licht dat je erin stuurt. De eigenschappen die ik daarbij bestudeerd heb zijn: de beste manier om dit soort materialen te maken, de temperatuursafhankelijkheid van de luminescentiesterkte en de levensduur van de luminescentie, dus hoe snel gaat het licht uit als de laser uit staat. De experimentele details en de resultaten die ik heb gevonden, staan beschreven in de rest van dit verslag.

Nu dan, het dankwoord. Als eerste wil ik Pieter Kik en Albert Polman bedanken. Van Pieter, mijn dagelijkse begeleider heb ik erg veel geleerd. Het (schijnbare?) gemak waarmee jij complexe dingen altijd doorzag en eenvoudige vragen kon stellen die mij weer dwongen over de simpelste dingen na te denken, is iets waar ik erg jaloers op ben!

Albert was altijd enthousiast en motiveerde daardoor mij ook extra, dat is erg leuk. Het belangrijkste dat ik van jou heb geleerd is: "Never believe it, until you see the data." Dit soort scepsis is, denk ik, erg belangrijk om een experiment goed te kunnen begrijpen. Verder wil ik je bedanken voor de mogelijkheid om twee maanden naar CERN in Genève te gaan, om daar eens te bekijken of de hoge-energie fysica het terein is waar ik zou willen werken. Ondanks dat ik dat toch niet ga doen, ben ik erg blij dat ik de kans had om die richting te onderzoeken.

Ik heb onderzoek doen in onze groep altijd als gezellig ervaren en vond het leuk dat we allemaal zo ons eigen onderzoeksgebiedje hebben binnen het geheel van de opto-electronics group. Ontspannen kletsend tijdens de pauzes, heb ik zo toch wel behoorlijk wat opgestoken van wat jullie doen en wat de problemen daarbij zijn. Bedankt allemaal, voor een gezellige tijd.

Tenslotte bedank ik Marieke, zonder jou was ik immers nooit zo ver gekomen.

ELSEVIER

Nuclear Instruments and Methods in Physics Research B 148 (1999) 497–501

NIM B
Beam Interactions with Materials & Atoms

Optical and electrical doping of silicon with holmium

J.F. Suyver [a,*], P.G. Kik [a], T. Kimura [a,1], A. Polman [a], G. Franzò [b], S. Coffa [b]

[a] FOM-Institute for Atomic and Molecular Physics, Kruislaan 407, 1098 SJ Amsterdam, The Netherlands
[b] CNR-IMETEM, Stradale Primosole 50, I-95121 Catania, Italy

Abstract

2 MeV holmium ions were implanted into Czochralski grown Si at a fluence of 5.5×10^{14} Ho/cm^2. Some samples were co-implanted with oxygen to a concentration of $(7\pm1)\times10^{19}$ cm^{-3}. After recrystallization, strong Ho segregation to the surface is observed, which is fully suppressed by co-doping with O. After recrystallization, photoluminescence peaks are observed at 1.197, 1.96 and 2.06 μm, characteristic for the $^5I_6\rightarrow{}^5I_8$ and $^5I_7\rightarrow{}^5I_8$ transitions of Ho^{3+}. The Ho^{3+} luminescence lifetime at 1.197 μm is 14 ms at 12 K. The luminescence intensity shows temperature quenching with an activation energy of 11 meV, both with and without O co-doping. The observed PL quenching cannot be explained by free carrier Auger quenching, but instead must be due to energy backtransfer or electron hole pair dissociation. Spreading resistance measurements indicate that Ho exhibits donor behavior, and that in the presence of O the free carrier concentration is enhanced by more than two orders of magnitude. In the O co-doped sample 20% of the Ho^{3+} was electrically active at room temperature. © 1999 Elsevier Science B.V. All rights reserved.

PACS: 61.72.T; 78.20.–e; 78.55.–m; 78.55.Ap
Keywords: Holmium; Luminescence; Rare earth; Silicon; Quenching; Doping

1. Introduction

The attainment of efficient light emission from silicon is of great importance to achieve integrated opto-electronic devices in which optical and electronic signal handling are performed on one Si chip. One way to achieve light emission from Si is by doping with rare earth ions. The trivalent (the preferred bonding state) ions have an incomplete 4f shell that is electrically shielded from the surrounding host material by filled 5s and 5p shells. This leads to relatively sharp and temperature independent intra 4f transitions. Doping of Si with erbium ions, that emit at 1.54 μm, an important telecommunication wavelength, has been studied extensively [1,2], and room temperature photo-and electroluminescence has been achieved [3,4]. While the emission at 1.54 μm from the Si:Er is important for the development of LED's, amplifiers and possibly lasers operating at 1.54 μm, one major disadvantage is that this wavelength cannot be detected by Si itself. It is therefore interesting to study doping with a rare earth ion that emits at a

* Corresponding author. Tel.: +31 20 608 1234; fax: +31 20 668 4106; e-mail: suyver@amolf.nl

[1] Present address: University of Electro-Communications, Tokyo, Japan.

0168-583X/98/$ – see front matter © 1999 Elsevier Science B.V. All rights reserved.
PII: S0168-583X(98)00807-6

smaller wavelength, such as holmium (Ho^{3+}). This ion has an optical transition from the second excited state ($^5I_6$) to the ground state ($^5I_8$) at 1.197 μm [5], close to the Si bandgap (see Fig. 1). At this wavelength the absorption coefficient of Si is 0.02 cm^{-1}. This means that both creation and detection of this wavelength on the same Si chip may be possible, thus allowing for the fabrication of an all-optical chip. In this paper the incorporation of Ho in Si by ion implantation and the first measurements of the optical and electrical properties are reported.

2. Experimental

A single crystal Czochralski-grown silicon wafer (⟨1 0 0⟩, P-doped, 1–5 Ω cm) was implanted with 2 MeV (5.5×10^{14} ions/cm^2) Ho ions at 77 K at a pressure below 10^{-6} mbar. Part of the wafer was co-implanted with oxygen at different energies (100, 187, 316 and 600 keV) to a total dose of 1.1×10^{16} ions/cm^2 in order to obtain a flat oxygen concentration profile. The average O concentration in the Ho implanted region measured with elastic recoil detection (ERD), was $(7\pm1)\times10^{19}$ O/cm^3. The amorphized Ho-doped (O-co-doped) layers were recrystallized by solid phase epitaxy (1 h at 490°C and 3 h at 600°C). Subsequently, rapid thermal annealing at 1000°C under flowing Ar atmosphere for 60 s was performed to anneal out residual damage and activate the implanted Ho atoms. Rutherford backscattering spectroscopy (RBS) using 2 MeV He^+ was used to measure Ho depth profiles, and recrystallization was examined by performing channeling measurements.

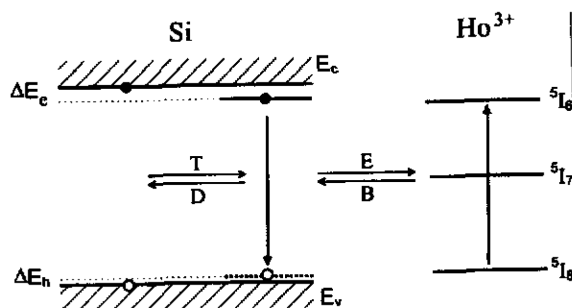

Fig. 1. Schematic model of trapping (T) and detrapping (D) of an exciton at a Ho related defect level and excitation (E) and energy backtransfer (B) of the Ho^{3+}.

Photoluminescence (PL) measurements were done using the 514.4 nm line of an Ar ion laser as a pump beam. The sample was mounted in a closed cycle helium cryostat, using silver paint to ensure good thermal contact. The PL signal was focused into a 96 cm monochromator and collected by a liquid nitrogen cooled Ge detector (wavelength range 1–1.6 μm) and a 2-stage thermoelectrically cooled PbS detector (1.6–2.3 μm). The spectra taken with the Ge detector were corrected for de-

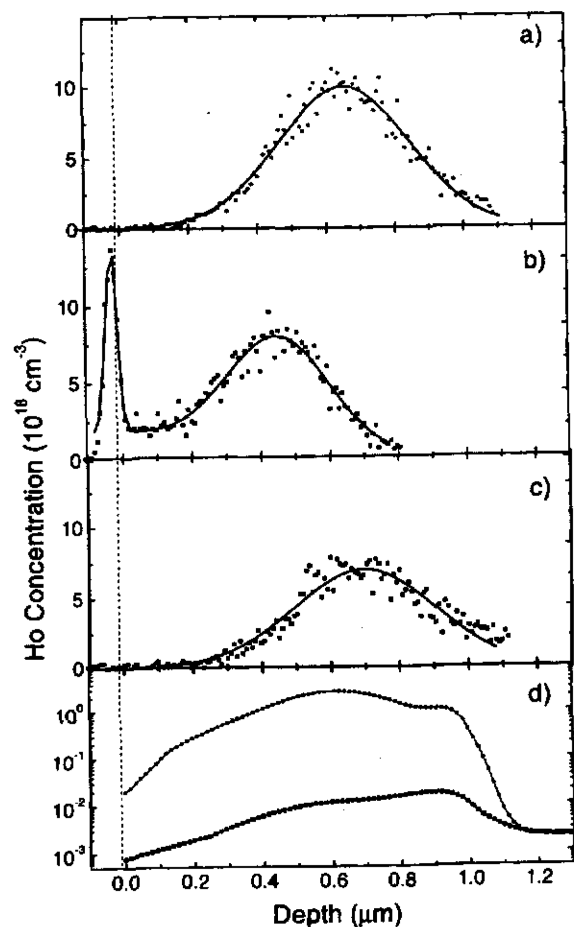

Fig. 2. RBS spectrum of Si:Ho before (a) and after (b) recrystallization and the spectrum of Si:Ho,O after (c) recrystallization. Also shown are SR profiles (d) of the Si:Ho sample (full circles) and the Si:Ho,O sample (open circles).

tector response. The signal was detected using standard lock-in techniques. Luminescence decay traces were obtained by averaging the detector signal on a digital oscilloscope. The system response time was 160 μs. Measurements were taken at temperatures ranging from 10 to 100 K.

The electrical properties of the Ho implanted layers were determined by room temperature spreading resistance (SR) measurements. The samples were beveled at an angle of 34′ and the spreading resistance data were converted into resistivity and carrier concentration using calibrated samples and a computational procedure by Berkowitz and Lux [6].

3. Results and discussion

Fig. 2 shows the Ho related signal of an RBS measurement before and after crystallization, with and without oxygen. The spectrum for the as-implanted sample (Fig. 2(a)) shows a Gaussian Ho distribution peaked at 650 nm with a full width at half-maximum of 250 nm. Channeling data (not shown) indicate that the Ho implantation causes amorphization of a 1.3 μm thick surface layer. After recrystallization (Fig. 2(b)) strong segregation of Ho to the surface was observed. This segregation is very similar to that observed previously for Er implanted Si, which was explained by a non-equilibrium segregation and trapping process, in which Er is segregated due to its low solubility in c-Si [7]. Fig. 2(c) shows the Ho profile of the O co-doped sample after recrystallization. In this case, no Ho segregation is observed. Again this is very similar to experiments on Si:Er,O. The absence of segregation is explained by the formation of strongly bound Ho–O clusters that are trapped in the growing crystal [7]. For all recrystallized samples, the channeling spectra of the Si showed good quality single crystal with a minimum yield of 5% after recrystallization.

In Fig. 2(d) carrier concentrations derived from spreading resistance data are shown for the Ho implanted sample with and without O. The background value in the bulk of the sample corresponds to the P doping of the Si. As can be seen, Ho implantation increases the carrier concentration to 2×10^{16} cm^{-3}. Co-implantation of O leads to a further increase in the free carrier concentration to a value of 3×10^{18} cm^{-3}. A similar effect was seen before in Si:Er,O [8]. From the absence of a p–n junction, it is concluded that the doping is n-type. Comparing the SR measurements with the RBS data, an upper limit for the electrically active fraction of Ho-ions of 20% was obtained for the O co-doped sample.

Fig. 3 shows a PL spectrum of the O co-doped sample taken at 12 K. For comparison the PL spectrum of Er-implanted CZ-Si (2 MeV Er, 2×10^{15} Er/cm^2, 2×10^{16} O/cm^3) is shown. A sharp PL peak is observed at 1.130 μm in the Ho-implanted sample, which is due to a phonon assisted band to band transition in Si [9]. In addition, a clear peak is observed at 1.197 μm, which corresponds to the $^5I_6 \rightarrow {^5I_8}$ transition of Ho^{3+} [5]. Furthermore, a broad luminescence band is observed for $\lambda > 1.2$ μm, which is attributed to defects remaining in the crystal after the implantation and annealing procedure [9]. The PL decay time of this background was measured to be <160 μs, as expected for defect luminescence. Two peaks in the long wavelength section of the spectrum, at 1.96 and 2.06 μm can be identified. The arrows in the figure indicate known wavelengths of the transitions between the Stark levels of the $^5I_7$ level and those of the $^5I_8$ level measured in e.g. oxide glasses

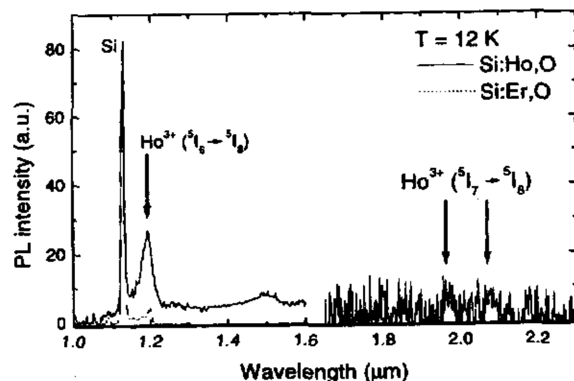

Fig. 3. PL spectrum of the Si:Ho,O sample, measured with a Ge detector ($\lambda < 1.6$ μm) and with a PbS detector ($\lambda > 1.6$ μm). Indicated by the arrows are literature values of the Ho^{3+} PL peaks [5]. The dashed line is a Si:Er,O spectrum with comparable Er and O concentrations.

[5]. They coincide with the measured peaks for the Ho-doped Si sample.

In Fig. 4, the temperature dependence of the luminescence at 1.197 μm is shown for both Ho-doped samples, with and without O. The Ho related intensity at each temperature was determined from the PL spectra by subtracting the background signal determined by interpolation of the intensities measured at 1.15 and 1.25 μm. As can be seen, both samples share an identical luminescence quenching behavior. The activation energy derived from the plot is 11 meV.

A luminescence decay trace measured at 1.197 μm at 12 K for the O co-doped sample is shown as an inset in Fig. 4. It shows a fast component that is detector-speed limited and is attributed to the background defect luminescence, and a slow component with a lifetime of 14 ms. Lifetimes in the 1–20 ms range are characteristic for rare earth ions in a variety of hosts [10]. The temperature dependence of the slow component of the lifetime was measured up to 25 K and is plotted (solid squares) in Fig. 4.

4. Ho excitation model

In general, the excitation of rare earth ions in Si is thought to occur through a mechanism indicated schematically in Fig. 1. An electron–hole pair is trapped (T) at a rare earth related defect level in the Si bandgap. Subsequently, the rare earth can be excited (E) by energy transferred through an impurity Auger process. Quenching processes in this model are energy backtransfer (B) from the excited rare earth to the defect state, and dissociation (D) of the electron hole pair. An additional quenching process of the Er population that was recently identified for Si:Er is Auger energy transfer to free carriers that are then excited higher in the conduction band [11].

Fig. 4 shows comparable luminescence quenching behavior with and without O while the carrier concentrations in these samples are very different (Fig. 2(d)). Note that Si:Er co-doped with high concentrations of P (with similar free carrier concentrations as in Fig. 1(d)) does show large Auger quenching. The difference between Si:Er and Si:Ho may be caused by a much smaller Auger coefficient or by a very large ionization energy of Ho, so that no free carriers are created up to 100 K. It is therefore concluded that the observed PL quenching in Fig. 4 is not due to Auger quenching to free carriers. This leaves only backtransfer and dissociation (see Fig. 1) as possible processes that could be the cause of the observed PL quenching.

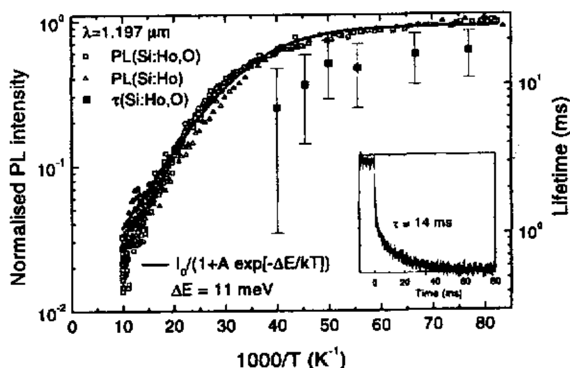

Fig. 4. Temperature dependence of the 1.197 μm PL intensity for the Si:Ho (triangles) and the Si:Ho, O (open squares) samples. Indicated with solid squares is the 1/e lifetime of the slow component of the 1.197 μm luminescence of the Si:Ho, O sample. The inset shows the corresponding decay trace measured at 12 K.

5. Conclusions

Ho implanted crystalline Si layers, (some co-doped with O) were regrown by solid phase epitaxy. Photoluminescence peaks are observed at 1.197, 1.96 and 2.06 μm, characteristic of the $^5I_6 \rightarrow {}^5I_8$ and the $^5I_7 \rightarrow {}^5I_8$ transitions of Ho^{3+}. Up to 100 K, the 1.197 μm luminescence of the Si:Ho and the Si:Ho,O samples quenches with temperature with a typical energy of 11 meV. The Ho^{3+} luminescence lifetime at 1.197 μm at 12 K is 14 ms. An increment of two orders of magnitude in the free carrier concentration is observed when samples are co-doped with O. It is concluded that the observed PL quenching is not caused by Auger quenching to free electrons, but rather by a backtransfer or an electron–hole dissociation process.

Acknowledgements

Wim Arnold Bik is acknowledged for his help in measuring oxygen profiles with ERD. This work is part of the Research Program of the Foundation for Fundamental Research on Matter (FOM) and was made possible by financial support from NWO, STW and the SCOOP program of the European Community.

References

[1] J. Michel, J.L. Benton, R.F. Ferrante, D.C. Jacobson, D.J. Eaglesham, E.A. Fitzgerald, Y.-H. Xie, J.M. Poate, L.C. Kimerling, J. Appl. Phys. 70 (1991) 2672.
[2] F. Priolo, G. Franzò, S. Coffa, A. Polman, S. Libertino, R. Barklie, D. Carey, J. Appl. Phys. 78 (1995) 3874.
[3] G. Franzó, F. Priolo, S. Coffa, A. Polman, A. Carnera, Appl. Phys. Lett. 64 (1994) 2235.
[4] B. Zheng, J. Michel, F.Y.G. Ren, L.C. Kimerling, D.C. Jacobson, J.M. Poate, Appl. Phys. Lett. 64 (1994) 2842.
[5] Sh.N. Gifeisman, A.M. Tkachuk, V.V. Prizmak, Opt. Spectrosc. (USSR) 44 (1978) 68.
[6] H.L. Berkowitz, R.A. Lux, J. Electrochem. Soc. 18 (1981) 1137.
[7] A. Polman, J.S. Custer, P.M. Zagwijn, A.M. Molenbroek, P.F.A. Alkemade, J. Appl. Phys. 81 (1997) 150.
[8] F. Priolo, S. Coffa, G. Franzò, C. Spinella, A. Carnera, V. Bellani, J. Appl. Phys. 74 (1993) 4936.
[9] G. Davies, Phys. Rep. 176 (1989) 83.
[10] A. Polman, J. Appl. Phys. 82 (1997) 1.
[11] F. Priolo, G. Franzò, S. Coffa, A. Carnera, Phys. Rev. B 57 (1998) 4443.

Holmium in amorphous Si:O, N, H

I. Introduction

Recently, it was shown that luminescence of the rare earth element holmium (Ho^{3+}) in Czochralski grown silicon (CZ-Si) can be obtained at the wavelengths 1.197 μm, 1.96 μm and 2.05 μm [1]. It is known for another rare earth element (erbium), that a significant increase in the photoluminescence (PL) intensity with respect to CZ-Si can be obtained by implantation in an oxygen-rich environment, such as semi-insulating polycrystalline / amorphous silicon (SIPOS) [2, 3]. This paper reports the first experimental data of Ho^{3+} luminescence in SIPOS and discusses thermal treatment and luminescence quenching.

II. Experimental

The semi-insulating polycrystalline silicon wafers are nonstoichiometric silicon oxide films deposited by plasma enhanced chemical vapor deposition on c-Si. These films were deposited at 250 °C and 900 mTorr with a flowrate of 28 standard cubic centimeter (sccm) SiH_4 and 347 sccm N_2O. Using a 500 keV van de Graaff accelerator, Ho was implanted to a total fluence of 6.3×10^{14} Ho/cm^2 into a 1.4 μm thick SIPOS layer at room temperature. Rutherford backscattering spectroscopy (RBS) using 2 MeV He^+ was used to measure the Ho depth profile and the SIPOS structure.

After implantation, the samples were annealed for 30 minutes in a vacuum furnace (base pressure 10^{-7} mbar) at temperatures of 200 °C, 300 °C or 400 °C. This was done to maximize the photoluminescence intensity of the Ho^{3+}. PL measurements were done using the 514.4 nm line of an Ar ion laser as a pump beam. The samples were mounted in a closed cycle helium cryostat, using silver paint to ensure good thermal contact. The PL signal was focused into a 96 cm monochromator and collected by a liquid nitrogen cooled Ge detector (wavelength range 0.9 μm – 1.8 μm) with a resolution of 2 nm. A long-pass filter (cut-off at 1120 nm) was used to remove the reflections of the Ar pump laser. The spectra taken with the Ge detector were corrected for detector response. The signal was detected using standard lock-in techniques.

III. Results and discussion

RBS showed a Gaussian Ho implantation profile that peaked at a depth of 240 nm and had a full with at half maximum of 150 nm. From the RBS data the SIPOS was found to consist of 1.4 μm $Si_{1.7}O_1N_{0.3}H_{0.2}$ (when the density is assumed to be ρ = 2.12 g/cm^3) on a Si substrate.

Figure 1 shows PL spectra of holmium implanted SIPOS for the different annealing treatments. The spectra were measured at 12 K using an average laser power of 0.5 mW on the sample, focused in a laser spot of 1 mm^2. Two distinct features can be observed in the spectra shown in figure 2. The first is a broad luminescence band that stretches from the filter cut-off at 1.12 μm up to ~ 1.4 μm. This luminescence band is most likely caused by the defect states present in the SIPOS and by luminescence of implantation induced defects. The broad luminescence band was found to extend to at least a wavelength of 1.0 μm in measurements without the long-pass filter (not shown). This is explained by noting that the bandgap of

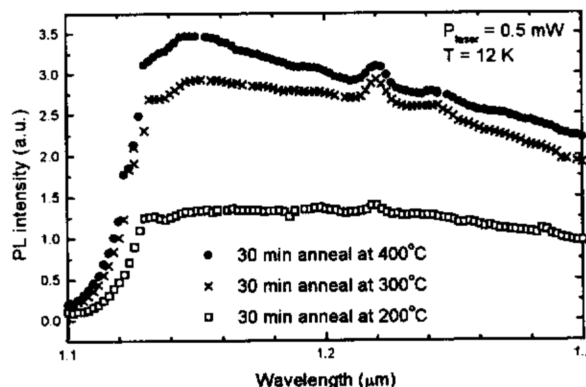

FIGURE 1: Photoluminescence spectra of SIPOS:Ho annealed for 30 minutes at 200 °C (□), 300 °C (x) and 400 °C (•). PL intensities may be compared.

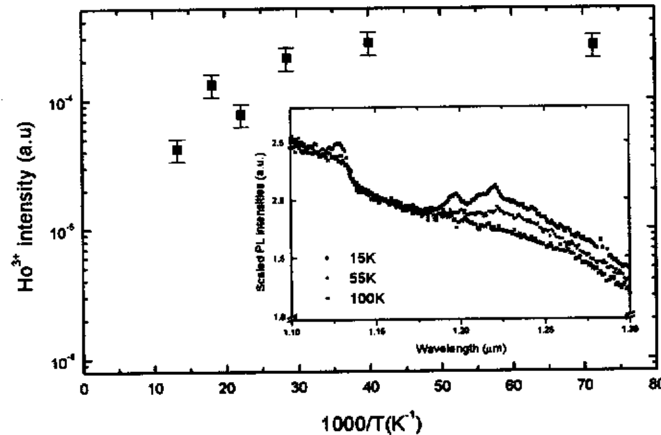

FIGURE 2: Quenching of the Ho related photoluminescence as measured at 1.22 μm. The inset shows PL spectra (normalized at 1.17 μm) taken at 15, 45 and 100 K.

SIPOS is larger than bandgap of Si at 1.1 μm.

The second feature is a luminescence peak at 1.22 μm. If this peak corresponds to the $^5I_6 \rightarrow {}^5I_8$ transition in Ho^{3+}, then a 20 nm (~17 meV) shift of the peak wavelength compared to CZ-Si has occurred [1]. However, literature shows both the values 1.22 μm (in $YAlO_3$ [4]) as well as 1.197 μm (in $LiYF_4$ [5, 6]) for this transition. This shift might be due to different Stark splitting in the host materials. When comparing the intensity of the peak at 1.22 μm in SIPOS:Ho with the peak at 1.2 μm in Si:Ho [1] (under identical experimental conditions and using the linear laser power dependence of the PL intensity at 1.2 μm), then it is noticed that the peak for SIPOS is 45 times stronger. Figure 1 also shows that the strength of the luminescence peak at 1.22 μm has a maximum for the sample annealed at 300 °C.

Figure 2 shows the Ho-related luminescence, derived by estimating the height of the peak in the PL spectrum. The background was interpolated linearly between 1.16 μm and 1.26 μm. The inset of figure 2 shows photoluminescence curves measured at 15 K, 45 K and 100 K respectively. For these PL measurements, a 900 nm long-pass filter was used and therefore the Si bandedge (at 1.13 μm) beneath the SIPOS is visible.

Earlier experiments on Si:Ho showed quenching of the Ho-related luminescence above 20 K [1]. However, from figure 2 it is clear that no significant quenching of the Ho-related luminescence for T < 40 K is found for SIPOS:Ho. In the case of Er luminescence, a similar lowering of the luminescence quenching going from Si to SIPOS is observed [2]. This is explained by the larger bandgap of SIPOS compared to Si and thus a larger distance from the $^5I_6$ level of Ho^{3+} to the conduction band. This larger distance results in less coupling to the conduction band and thus less quenching of the Ho^{3+} luminescence.

IV. Conclusions and acknowledgments

Implantation of 6.3×10^{14} Ho/cm^2 into SIPOS and subsequent annealing at 200 °C, 300 °C or 400 °C resulted in the first evidence of Ho^{3+} luminescence at 1.22 μm in SIPOS. A maximum of the Ho^{3+} related luminescence was found for an anneal temperature of 300 °C. The background corrected Ho-related luminescence curve at 1.22 μm for the sample annealed at 300 °C showed little quenching below 50 K. At higher temperatures quenching was observed. The Ho-related luminescence was found to be 45 times stronger than in Si.

The author would like to thank Mark Brongersma for useful comments.

References

[1] J. F. Suyver, P. G. Kik, T. Kimura and A. Polman, G. Franzò and S. Coffa, Nucl. Instr. and Meth. in Phys. Res. Sect. B **148**, 497 (1999).

[2] G. N. van den Hoven, J. H. Shin and A. Polman, S. Lombardo and S. U. Campisano, J. Appl. Phys. **78**, 2642 (1995).

[3] S. Lombardo and S. U. Campisano, G. N. van den Hoven and A. Polman, J. Appl. Phys. **77**, 6504 (1995).

[4] A. A. Kaminskii, Sov. Phys. Dokl. **31**, 832 (1986).

[5] S. N. Gifeisman, A. M. Tkachuk and V. V. Prizmak, Opt. Spectrosc. (USSR) **44**, 68 (1978).

[6] B. M. Walsh, N. P. Barnes, B. Di Bartolo, J. Appl. Phys. **83**, 2772 (1998).

Energy transfer in Si:Er *p-n* diodes

I. Introduction

There exists a large interest in semiconductors doped with rare earth ions because of the possible applications in opto-electronic devices. Rare earth ions in their trivalent form have well defined intra *4f* energy transitions because the partially filled *4f* shell is surrounded by filled *5s* and *5p* shells. The energy transfer through the Si:Er system has been the subject of study for several years and is believed to take place through the energy levels and rates indicated schematically in figure 1 [1]. Most of the research until today focuses on the photoluminescence (PL) of Er^{3+}, excited through optically or electrically generated carriers in the Si. Recently, measurements have become available of the reverse process, in which an electron-hole pair is generated upon the optical excitation of the Er^{3+} ion. When the Er^{3+} ion is placed inside a *p-n* junction, a current can be detected when the structure is illuminated with 1.53 μm light. The structure used was a passivated-emitter rear-locally defused (PERL) Si solar cell, fabricated at the university of New South Wales (Australia). It had a textured surface to enhance the light-trapping in the cell.

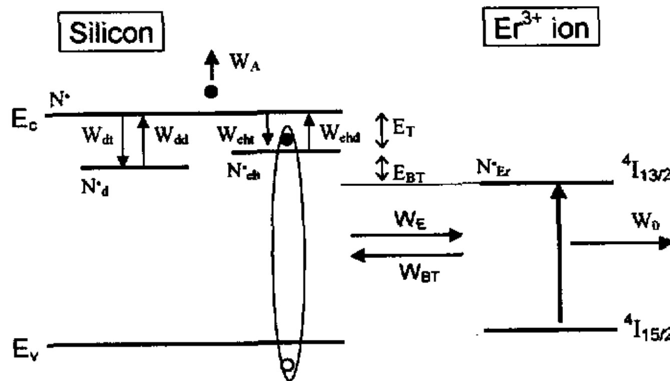

FIGURE 1: Schematic representation of the Si:Er system. Shown in this figure are the transfer rates (W_i) and the populations of the levels (N^*_i).

In the photocurrent generation process, an Er^{3+} ion can be optically excited (population: N^*_{Er}) using a 1.53 μm photon, at a generation rate g_{Er}. This excitation can transfer its energy via a backtransfer process (at a rate W_{BT}) to form a bound electron-hole pair at an Er-related defect level (this population is denoted by N^*_{eh}). Other energy transfer processes for an excited Er ion are Auger quenching to a free carrier (W_A) or decay by emitting a photon (W_0). An electron-hole pair in the N^*_{eh} level can detrap and transfer its energy to the conduction band (W_{ehd} and population N^*) or excite the Er^{3+} ion (W_E). Once an electron-hole pair is at the bandedge, then this electron-hole pair can be detected using a *p-n* junction in which the electron-hole pair gets separated and collected (with a collection rate C_0) in the form of a current. Other processes that can occur are the trapping of an exciton at an Er-related defect level (W_{eht} and population N^*_{eh}), or trapping at a defect level (W_{dt}) not coupled to Er with a population N^*_d. At this defect level, an exciton can also be generated optically, with a generation rate g_d. The assumption is made that this defect-bound exciton has only one possible decay path: detrapping to the conduction band (W_{dd}).

Measurements have been performed of the photocurrent and the photoluminescence intensity at 1.535 μm of Er^{3+} ions implanted in a *p-n* junction as a function of temperature. The experimental data taken from ref. [2] are shown in figure 2. Figure 2a shows the temperature dependence of the photocurrent under 1.535 μm illumination (6 mW, 1.5 cm^2 spot). The photocurrent increases over two orders of magnitude as the temperature is increased from 90 K to 300 K. Figure 2b also shows the PL intensity at 1.535 μm, measured on the same sample. The PL intensity decreases weakly with increasing temperature up to 120 K and a strong temperature quenching is observed above 150 K.

Note that the photocurrent (I_γ) scales linearly with the concentration of free electrons (N^*) in the depletion region: $I_\gamma \propto N^*$. Similarly, the photoluminescence intensity (I_{PL}) scales with the population of excited Er^{3+}: $I_{PL} \propto N^*_{Er}$. In this paper, a rate equation model will be presented that simultaneously describes the temperature dependence of the photocurrent and photoluminescence data. The impact that several parameters in the rate equation model have on the behavior of the photocurrent and photoluminescence as a function of temperature will be shown and discussed.

II. Model

From the rate constants attributed to all energy transfer processes shown in figure 1, the four coupled differential equations that describe the Si:Er system in a *p-n* junction can be found

$$\partial_t N^* = W_{ehd} N^*_{eh} - W_{eht} N^* + W_{dd} N^*_d - W_{dt} N^* - C_0 N^*$$

$$\partial_t N^*_{eh} = W_{eht} N^* - W_{ehd} N^*_{eh} + W_{BT} N^*_{Er} - W_E N^*_{eh}$$

$$\partial_t N^*_{Er} = W_E N^*_{eh} + g_{Er} N_{Er} - (W_{BT} + W_0 + W_A) N^*_{Er}$$

$$\partial_t N^*_d = g_d (N_d - N^*_d) - W_{dd} N^*_d + W_{dt} N^*$$

where the assumption is made that the fraction of excited Er^{3+} and the population N^*_{eh} are small. Furthermore, the photoluminescence that is measured is assumed to originate from Er ions located inside the depletion region. This system of equations was solved analytically in the steady state case ($\partial_t N^*_i = 0, \forall i$) using the symbolic computer algebra program *Mathematica 3.0*.

The generation rate constants are given by

$$g_E(T)_r = B\, \sigma_{Er}(T)\, \phi \qquad \text{and} \qquad g_d = B\, \sigma_{do}\, \phi$$

where ϕ denotes the laser flux, σ_i the cross-section for optical excitation and B the product of the transmission coefficient for the 1.53 μm light into the *p-n* junction and the number of internal reflections in the Er-doped Si junction. The collection rate for a 1 μm wide depletion region with an electric field of 10^4 V/cm is estimated to be $C_0 = 3.3 \times 10^{11}\ s^{-1}$.

The Er optical absorption cross-section is temperature dependent due to the Boltzmann distribution over the Stark-split levels of the Er^{3+} *groundstate. By determining* the ratio of the PL peak value at 1.535 μm to the integrated photoluminescence spectrum, a measure for the temperature dependent value for the optical absorption cross section of Er^{3+} has been obtained [2]. This resulted in

$$\sigma_{Er}(T) = \sigma_{Er}(300)[cm^2] \times \left(0.99 + 0.71 \times e^{-0.015\ T[K]}\right)$$

The value of the cross section at 300 K was taken to be $\sigma_{Er}(300\ K) = 6 \times 10^{-20}\ cm^2$ [2]. From the measured photoluminescence lifetime at 15 K (1 ms) a value of $W_0 = 10^3\ s^{-1}$ was derived. The next section discusses the rate constants used in the model described in this section and points out the fitting parameters that influence the solutions of the rate equations.

II.a. Fitting parameters

De-excitation of an excited Er ion can take place via Auger energy transfer to a free carrier (W_A). The Auger rate is determined by the concentration of free carriers and a coupling constant C_A [3], this gives

$$W_A(T) = C_A \sqrt{\tfrac{1}{2} N_{don} N_c}\; e^{-\frac{E_A}{2kT}}$$

where N_{don} is the donor concentration, which is unknown. Therefore N_{don} is used as a fitting parameter. The other parameters are known materials properties: N_c is the (temperature dependent) density of states at the bottom of the conduction band [4] and C_A is the Auger coefficient, which was recently measured [5]. Finally, E_A = 25 meV, the ionization energy the Er-related donor level in Czochralski-grown Si [9].

The temperature dependence of the energy backtransfer rate can be written as an activated process, [3]

$$W_{BT}(T) = W_E e^{-\frac{E_{BT}}{kT}}$$

where E_{BT} is the backtransfer activation energy which is known to be 135-150 meV [6] and W_E is a transfer rate. In this paper, the value E_{BT} = 150 meV is used.

The Er-related exciton trapping and detrapping rates are determined by the trapping cross-section, the thermal velocity v(T), the density of states and (in the detrapping case) an activation energy for detrapping to the conduction band

$$W_{eht}(T) = \sigma_{eh}\, v(T)\, N_c(T) \qquad \text{and} \qquad W_{ehd}(T) = \sigma_{eh}\, v(T)\, N_c(T)\, e^{-Eeh/kT}$$

where $E_{eh} = E_{gap} - E_{Er} - E_{BT}$ = 150 meV. The defect (de)trapping rates are written similar to the exciton (de)trapping rates

$$W_{dt}(T) = \sigma_d\, v(T)\, N_c(T) \qquad \text{and} \qquad W_{dd}(T) = \sigma_d\, v\, N_c(T)\, e^{-Ed/kT}$$

with E_d = 10 meV as a typical exciton binding energy [4]. The two cross-sections σ_{eh} and σ_d could be used as fitting parameters.

The last parameter that is used in the fitting process is the defect density, N_d, which (in contrast to the Er density N_{Er}) could not be measured. It is known that there exist types of defects, for which the active defect concentration is temperature dependent and can be written as [7]

$$N_d(T) = N_{d0}\, e^{-Edefect/kT}$$

where N_{d0} and E_{defect} are used as fitting parameters. Incorporation of this type of defects in the model is required to explain the observed behavior of the photocurrent as a function of temperature for two reasons: (1) Photocurrent spectra taken at temperatures < 300 K indicate that a large fraction of the photocurrent is not related to Er (50 % at 300 K). (2) The temperature dependence of the photocurrent below 200 K can not be explained by the Er backtransfer only (given its activation energy of 150 meV).

II.b. Fitting results

Calculations of the photocurrent (I_γ) and photoluminescence (I_{PL}) data are shown in figure 2 (solid line). The parameters that were used to obtain this fit are listed in the left column of table 1. The right column lists the known material parameters used in the calculation. For the photocurrent fit, the separate contributions of the defects ($I_\gamma^{(defect)}$, □) and of the Er ions ($I_\gamma^{(Er)}$, x) are shown. Excellent agreement between experimental data and the fit is obtained, showing that the proposed model can indeed simultaneously describe the photoluminescence and photocurrent data.

Parameter	Value
N_{don}	3.0×10^{13} cm^{-3}
W_E	1.6×10^{8} s^{-1}
σ_{eh}	8.1×10^{-16} cm^{2}
E_{defect}	60 meV
$\sigma_d N_{d0}$	5.4×10^{-1} cm^{-1}
σ_{d0}	> 10^{-23} cm^{2}
B	4.5

Parameter	Value
E_{BT}	150 meV
C_A	5×10^{-13} cm^{3}s^{-1}
$\sigma_{Er}(300)$	6×10^{-20} cm^{2}
C_0	3.3×10^{11} s^{-1}
W_0	10^{3} s^{-1}
ϕ	1.16×10^{17} cm^{-2}s^{-1}

Table 1: Values of the fitting parameters (left) with which the best fitting result was obtained and of the known material parameters (right). See figure 2 for the associated plots.

The values for the trapping cross-section σ_{eh} shown in table 1 is comparable to other experimental data on cross-sections [8]. The values of σ_d and N_{d0} are interchangeable and thus only their product is relevant (as will be discussed in section III.d.). The product $\sigma_d N_{d0}$ yields an acceptable order of magnitude for the defect density (10^{14} cm^{-3}) if the cross-section

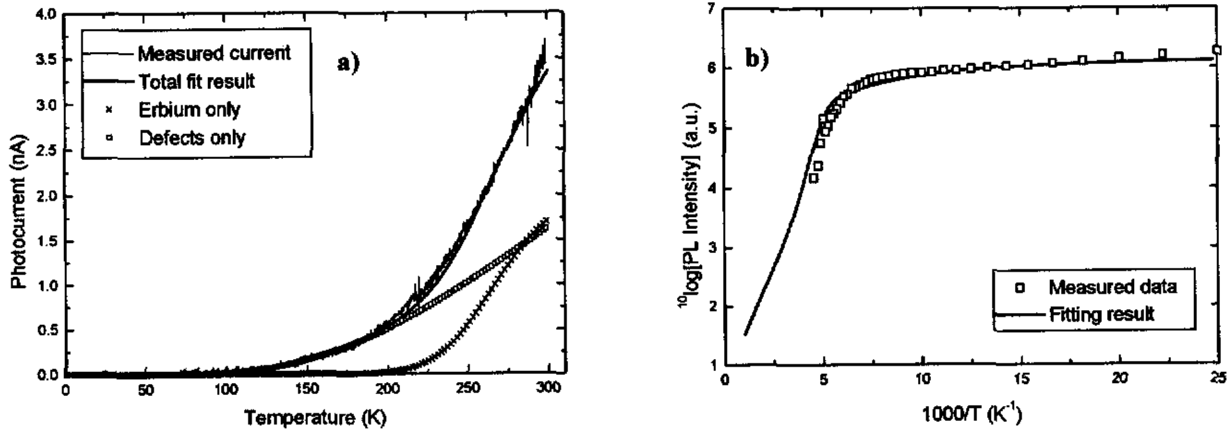

FIGURE 2: a) Best fit (thick line) of the photocurrent and b) the photoluminescence intensity data using the model described in the text. Also shown are the separate contributions of the Er^{3+} (x) and the defects (□) for the photocurrent fit. Data taken from ref [2].

is taken in the order of 10^{-15} cm^2. The rate constant W_E is also comparable with the known literature value [6]. The value found for the donor concentration ($N_{don} = 3 \times 10^{13}$ cm^{-3}) is much lower than the implanted Er density (peak concentration 10^{17} cm^{-3}). This is attributed to the fact that not all the Er is electrically active and that the carrier density in the depletion region is very low.

Figure 2a shows a comparison between the calculations and experimental data of the photocurrent in nA. The scaling factor B (the product of the transmission coefficient and the number of internal reflections in the Er-doped Si junction) changes the height of this curve. Fitting yielded a value of 4.5 for B as shown in table 1 (left). This implies (assuming high transmission into the *p-n* junction) that the light will reflect ~5 times inside the junction.

Because there exists a possibility for electron retrapping at either an Er-related defect level or a defect site, there will be coupling between the N^*_{Er} and the N^*_d populations. Therefore $I_\gamma \neq I_\gamma^{(Er)} + I_\gamma^{(defect)}$, but because the collection rate is much larger than the retrapping rate, the difference is very small: $(I_\gamma - I_\gamma^{(Er)} - I_\gamma^{(defect)}) < 10^{-4}$ nA.

When the parameters that resulted from the fitting procedure are incorporated into the model, then it is noticed that for all temperatures $N^*_{eh}/N_{Er} < 10^{-6}$ and $N^*_{Er}/N_{Er} < 10^{-3}$. This shows that up to the pump power conditions used in this experiment, no saturation is to be expected, which agrees with the assumption that was made in section II. Furthermore, a value of all the rates depicted in figure 1 can now be calculated at every temperature. Table 2 shows values of these rates at 15 K and at 300 K.

	15 K	300 K
W_0	1.0×10^3	1.0×10^3
W_A	7.5×10^{-3}	6.5×10^3
W_{BT}	6.1×10^{-43}	4.8×10^5
W_E	1.6×10^8	1.6×10^8
W_{eht}	5.1×10^6	2.3×10^7
W_{ehd}	2.8×10^{-44}	8.8×10^6
W_{dt}	2.5×10^7	1.1×10^8
W_{dd}	3.2×10^3	2.0×10^9
C_0	3.3×10^{11}	3.3×10^{11}

Table 2: Rates (s^{-1}) of the energy transfer processes at 15 K and 300 K.

Table 2 shows that at 15 K $W_{BT} \approx 0$ and $W_{ehd} \approx 0$, which implies that no Er-related current should be observable. This agrees with the measured photocurrent (figure 2). For high temperatures (such as 300 K), it is noted that $\{W_{BT}, W_{ehd}\} >> W_0$. This implies that at high temperatures $I_{PL} \rightarrow 0$ as is observed. The fact that at high temperatures $\{W_{BT}, W_{ehd}\} >> W_A$ means that the generation of photocurrent will become the dominant Er^{3+} de-excitation path.

III. Trends from the model

In section II.a six parameters that influence the calculations were discussed: σ_{eh}, N_{don}, W_E, σ_d N_{d0}, E_{defect} and σ_{do}. In this section, the effect of these parameters on the solutions of the model presented in section II are discussed.

The following plots will show trends in the photoluminescence and the photocurrent as a function of temperature. In these plots, the population of free electron-hole pairs (N^*) as a function of temperature and the logarithm of the population of excited Er ions (N^*_{Er}) as a function of 1000/T is shown. In all the graphs shown in this section, only one of these parameters is varied. The others are set to the values obtained in section II.b. This presentation of the calculations was chosen because the trends in the calculations are most clearly visible this way.

III.a. Electron-hole trapping cross-section

Figure 3 shows the behavior of photocurrent and of the photoluminescence intensity for different values of σ_{eh}. This parameter describes the coupling between the free electron-hole population (N^*) and the Er-related defect population (N^*_{eh}). The values used for this parameter were 10^{-19} cm^2 (□), 10^{-16} cm^2 (x) and 10^{-14} cm^2 (•).

Increasing the value of σ_{eh} leads to a significant increase of I_γ and a decrease of I_{PL} at temperatures higher than 175 K. Both effects are due to the higher electron-hole detrapping rate (W_{ehd}) which scales linearly with σ_{eh}: a faster detrapping rate to the conduction band for an excited Er^{3+} ion (due to the larger cross-section) results in a lower population N^*_{Er} (and a lower I_{PL}) and a higher population N^* (and a higher I_γ).

III.b. Auger quenching and donor density

Figure 4 shows the dependence of the calculations on the donor density that is included in the Auger rate. The parameter N_{don} was varied over seven orders of magnitude. The values that were used for this parameter were 3×10^9 cm^{-3} (□), 3×10^{13} cm^{-3} (x) and 7×10^{16} cm^{-3} (•).

Increasing the value of N_{don} results in a decrease of I_{PL} and I_γ. This is explained by the fact that an increase in the Auger rate leads to a decrease of the population of excited Er ions, without the generation of photons or current.

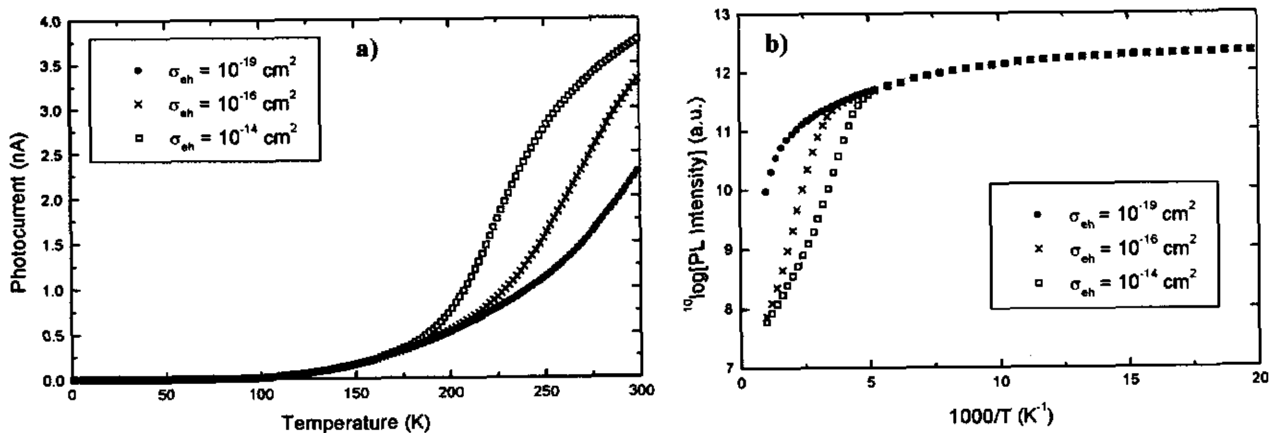

FIGURE 3: Three calculations of the photocurrent (a) and the photoluminescence intensity (b) for different values of the electron-hole trapping cross-section, σ_{eh}.

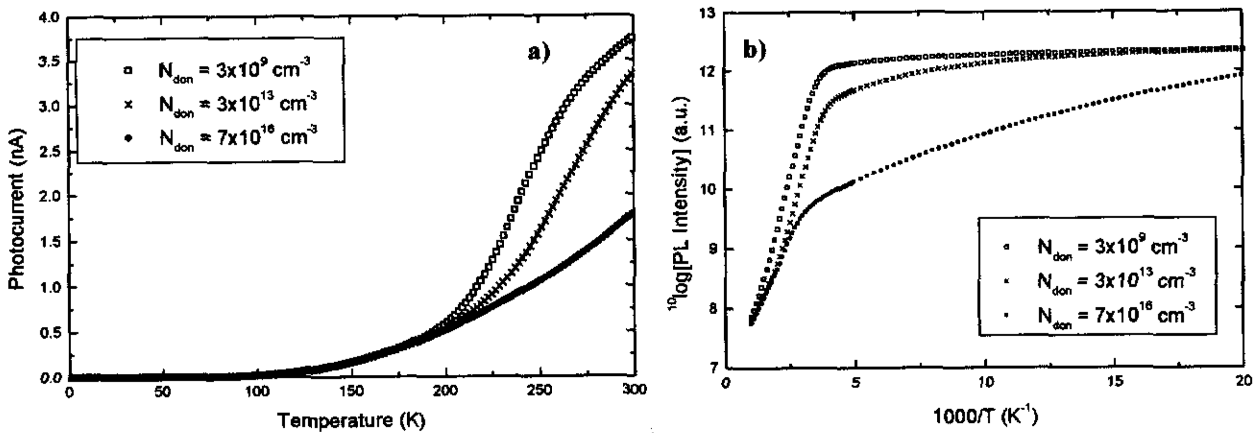

FIGURE 4: Results of variations of the donor density N_{don} on the photocurrent (a) and the photoluminescence intensity (b) using the model described above.

III.c. Excitation rate

Figure 5 shows the behavior of $I_γ(T)$ and of $^{10}\log[I_{PL}(1000/T)]$ while changing the excitation rate W_E over six orders of magnitude. This rate describes the coupling between the Er level and the Er-related defect level. The values 10^3 s^{-1} (□), 10^6 s^{-1} (x) and 10^9 s^{-1} (•) were used for this calculation.

Figure 5 shows that for temperatures above 200 K, an increase of W_E leads to an increase of $I_γ$ and a decrease of I_{PL}. This behavior can be explained by realizing that a smaller value of W_E will lower the rate from an excited Er^{3+} to the trapped electron-hole state (and therefore lower $I_γ$). This means that more excitations result in photoluminescence, leading to an increase of I_{PL}.

III.d. Density of defects

Figure 6 shows the behavior of the model curves when the parameter N_{d0} is changed. The values 10^{12} cm^{-3} (□), 10^{14} cm^{-3} (x) and 10^{16} cm^{-3} (•) were used for N_{d0}.

At temperatures above 50 K, the increase in the number of (active) defects results in an increase of $I_γ$ and does not influence I_{PL}. The increase in $I_γ$ is due to the larger number of active defects, which all contribute to the defect-related current. The fact that I_{PL} does not change shows that carriers produced at the defects do not retrap at an Er-related defect level. Therefore nearly all of the population N^* is converted into photocurrent.

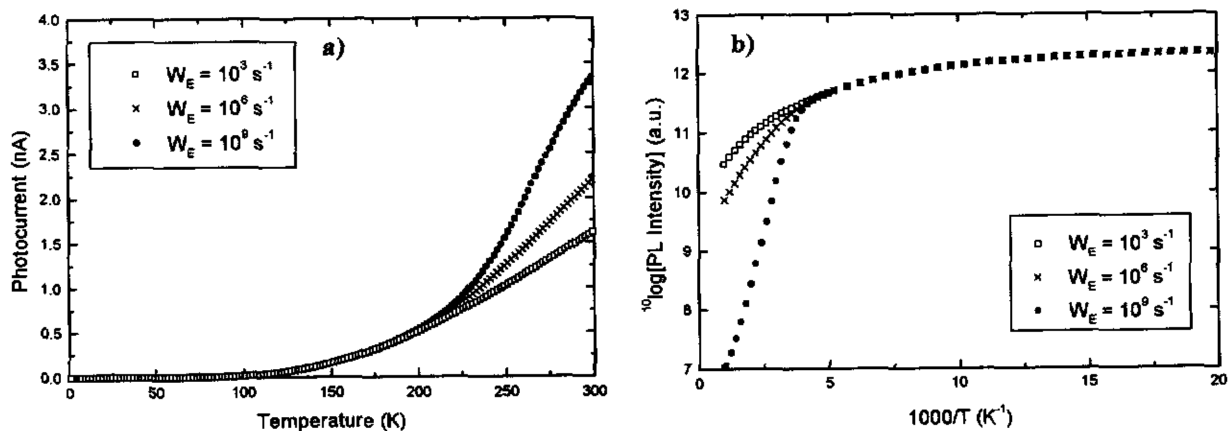

FIGURE 5: Photocurrent (a) and the photoluminescence intensity (b) curves using the model described above while varying the fitting parameter W_E.

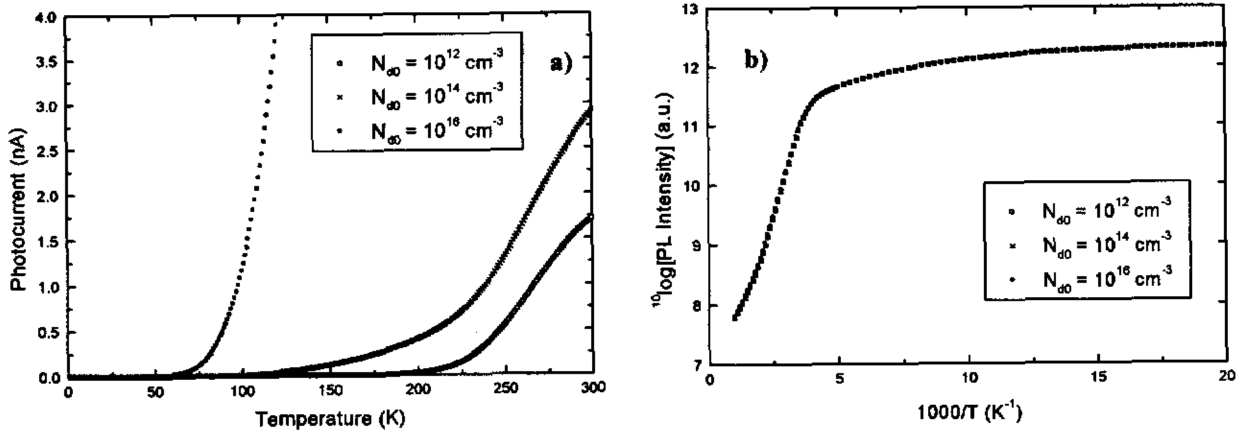

FIGURE 6: Model fits showing results of variations of the density of defects (N_{d0}) on the photocurrent (a) and the photoluminescence intensity (b).

The value of σ_d was also changed and an identical trend was observed. From this, the conclusion is drawn that the total number of defects N_{d0} and the electrical absorption cross-section for defects σ_d cannot be fitted separately, because only their product is relevant. This is explained by the fact that at low temperature all the defects are excited ($N^*_d \rightarrow N_d$) and therefore increasing N_{d0} and simultaneously decreasing σ_d by the same factor will not change any results from the calculations.

III.e. Activation energy of defects

Figure 7 shows the dependence of the calculation of the photocurrent on the activation energy of the defects. The values used for this parameter were 10 meV (□), 50 meV (x) and 100 meV (•).

Because of the negligible coupling between the N^*_d level and the N^*_{Er} level, no effect on the calculation of the photoluminescence intensity was found (not shown). Increasing the activation energy of the defects leads to a decrease of the number of activated defects. Since at low temperatures (when W_{dd} is very small) all the activated defects are filled, a decrease of the number of activated defects will lead to a decrease of the photocurrent.

III.f. Optical cross-section for not Er-related defects

The calculations of the model showed no change in I_{PL} or I_γ for reasonable values of the optical cross-section (> 10^{-22} cm^2) for photon capture at a defect. However, using

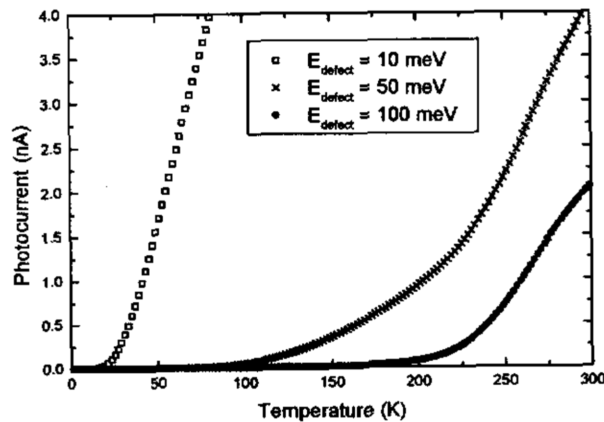

FIGURE 7: Effects of the fitting parameter E_{defect} on the photocurrent solutions from the model.

extremely small vales of σ_{do} (~10^{-30} cm^2) results in a change of the calculated photocurrent behavior. This is explained through the fact that $g_d = \sigma_{do}\ \phi$. When the optical cross-section is so small that the generation rate becomes the rate-limiting step (instead of the defect detrapping rate W_{dd}) to create current via a defect, then a change in the photocurrent spectrum will become observable.

IV. Conclusions

The main result from the work described in this paper is that the described model for the energy transfer works very well. The photocurrent and the photoluminescence intensity solutions from the model can be influenced using the parameters W_E, N_{don}, $\sigma_d\ N_{d0}$ and E_{defect}. Within reasonable values of the parameter σ_{do} (> 10^{-22} cm^2), no changes in the solutions of the model were observed at all.

A very good fit of both the photocurrent and the photoluminescence data was obtained from the model. To obtain this fit, the values $N_{don} = 3\mathrm{x}10^{13}$ cm^{-3}, $W_E = 1.6\mathrm{x}10^8$ s^{-1}, $\sigma_{eh} = 8.1\mathrm{x}10^{-16}$ cm^2, $\sigma_d\ N_{d0} = 5.4\mathrm{x}10^{-1}$ cm^{-1}, $\sigma_{do} > 10^{-22}$ cm^2 and E_{defect} = 60 meV were used.

Acknowledgements

The author would like to thank Nick Hamelin and Kostya Kikoin for valuable discussions that contributed to this work.

References

[1] S. Coffa, G. Franzò and F. Priolo, A. Polman and R. Serna, Phys. Rev. B **49**, 16313 (1994); A. Polman, G. N. van den Hoven, J. S. Custer, J. H. Shin and R. Serna, P. F. A. Alkemade, J. Appl. Phys. **77**, 1256 (1995); G. Franzò and S. Coffa, F. Priolo, C. Spinella, J. Appl. Phys. **81**, 2784 (1997).

[2] N. Hamelin, J. F. Suyver, P. G. Kik, K. Kikoin and A. Polman, A. Schönecker and F. W. Saris, M. A. Green, to be published.

[3] J. Palm, F. Gan, B. Zheng, J. Michel and L. C. Kimerling, Phys. Rev. B **54**, 17603 (1996).

[4] S. M. Sze, *Physics of Semiconductor Devices* (John Wiley & Sons, New York, 1981).

[5] F. Priolo, G. Franzò and S. Coffa, A. Carnera, Phys. Rev. B **57**, 4443 (1998).

[6] P. G. Kik, M. J. A. de Dood, K. Kikoin and A. Polman, Appl. Phys. Lett. **70**, 1721 (1997).

[7] W. Shockley, *Electrons and Holes in Semiconductors* (D. van Nostrand, Princeton, N.J. 1950).

[8] S. Libertino, S. Coffa, G. Franzò and F. Priolo, J. Appl. Phys. **78**, 3867 (1995).

[9] L. Palmetshofer, Yu. Suprun-Belevich and M. Stepikhova, Nucl. Instr. And Meth. B **127/128**, 479 (1997).

Abstract for NeVac, April 3 1998, Venlo.

Optical and electrical doping of silicon with holmium

J.F. Suyver, P.G. Kik, T. Kimura, and A. Polman
FOM-Institute for Atomic and Molecular Physics
Kruislaan 407, 1098 SJ Amsterdam

The attainment of efficient light emission from silicon is important to achieve integrated opto-electronic devices in which optical and electrical signal handling are combined on one Si chip. The rare earth ion holmium is an interesting dopant in Si as it has an optical transition at 1.18 μm, close to the bandgap of Si. At this wavelength the absorption depth of Si is small enough for light to propagate over an appreciable length in a Si-based waveguide. As the holmium transition energy is less than the Si bandgap energy, holmium ions in Si may be excited electrically.

Holmium ions were implanted at room temperature in Czochralski-grown Si(100) at 500 keV ($5x10^{14}$ ions/cm^2) or 2 MeV ($1.2x10^{15}$ ions/cm^2). Some samples were co-implanted with oxygen at a dose of $5x10^{15}$ or $5x10^{16}$ ions/cm^2. Annealing at 490 °C and 600 °C causes recrystallizion of the amorphized surface layer, as shown by Rutherford backscattering spectroscopy.

Photoluminescence spectroscopy at 13 K using an Ar^+ pump laser at 514.4 nm shows a clear peak around 1.18 μm, which may be attributed to the $^5I_6 \rightarrow ^5I_8$ transition in Ho^{3+}. The transition shows a lifetime as long as 15 ms, characteristic for a rare earth ion. Increasing the sample temperature to 100 K, a quenching of the luminescence intensity with characteristic activation energy of 25 meV is observed. Spreading resistance measurements were performed to determine the carrier depth profiles in these samples. It is found that O co-doping leads to a three orders of magnitude enhancement of the fraction of electrically active Ho ions.

Optical and electrical doping of silicon with holmium

J.F. Suyver, P.G. Kik, T. Kimura and A. Polman
FOM-Institute for Atomic and Molecular Physics
Amsterdam, The Netherlands
G. Franzó and S. Coffa
CNR-IMETEM, Catania, Italy

The attainment of efficient light emission from silicon is important to achieve integrated opto-electronic devices in which optical and electrical signal handling are combined on one Si chip. The rare earth ion holmium is an interesting dopant in Si as it has an optical transition at 1.19 μm, close to the bandgap of Si. At this wavelength the absorption depth in Si is large enough for light to propagate over an appreciable length in a Si-based waveguide. As this holmium transition energy is less than the Si bandgap energy, holmium ions in Si may be excited electrically.

Holmium ions were implanted at room temperature in Czochralski-grown Si(100) at 500 keV (5×10^{14} ions/cm^2) or 2 MeV (1.2×10^{15} ions/cm^2). Some samples were co-implanted with oxygen at doses of 5×10^{15} or 1×10^{16} ions/cm^2. The amorphized Ho-doped layers were recrystallized by solid phase epitaxy at 600 °C. Spreading resistance measurements suggest that O co-doping increases the donor activity of holmium by three orders of magnitude.

The photoluminescence spectrum measured at 13 K using excitation at 514.4 nm shows a clear peak around 1.19 μm, which may be attributed to the $^5I_6 \rightarrow {^5I_8}$ transition in Ho^{3+}. The transition shows a lifetime as long as 15 ms, characteristic for rare earth luminescence. Increasing the temperature to 100 K, a quenching of the luminescence intensity with a characteristic activation energy of 9 meV is observed. A model will be presented that describes the luminescence behavior.

Optical and electrical doping of silicon with holmium

J.F. Suyver[a)], P.G. Kik[a)], T. Kimura[b)], G. Franzò[c)], S. Coffa[c)] and A. Polman[a)]

[a)] *FOM-Institute for Atomic and Molecular Physics, Kruislaan 407, 1098 SJ Amsterdam*

[b)] *University of Electro-Communications, Tokyo, Japan*

[c)] *CNR-IMETEM, Stradale Primosole 50, I-95121 Catania, Italy*

Introduction

Optical signal transmission is becoming more important, because of its large bandwidth. Applications such as on-chip timing signals require integration of optical and electrical components on a single chip.

To obtain high transmission of a signal through a crystalline Si chip, the photon energy has to be less than the Si bandgap (λ_{light} > 1.13 μm).

The rare earth ion holmium (Ho^{3+}) could serve as a light source: it has optical transition at 1.197, 1.96, 2.06 μm.

Sample preparation

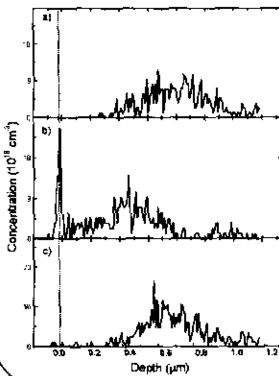

a) 2 MeV Ho (1.2x10^{15} cm^{-2}) was implanted in *n*-type, P-doped CZ-Si. RBS shows a Gaussian Ho peak at 700 nm and FWHM of 300 nm.

b) SPE at 600 °C to recrystallize. Ho segregation to the surface is observed.

c) Implantation as a), but also (7±1)x10^{19} O/cm^3 is implanted. No segregation of Ho is observed after SPE.

Photoluminescence spectroscopy

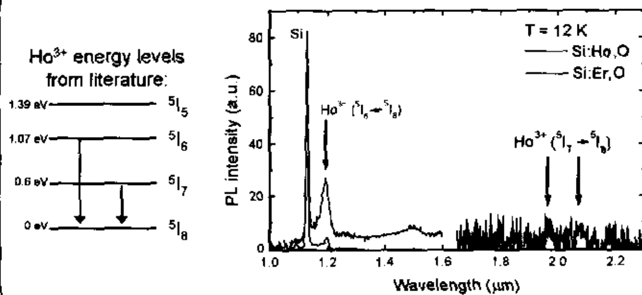

Ho^{3+} has no absorption near 514.4 nm ⇒ Electrical excitation of Ho^{3+}.

Luminescence decay

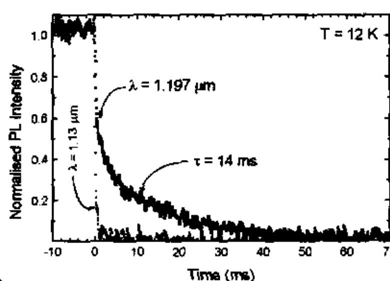

Luminescence decay at 1.197 μm is composed of a fast component (attributed to defect background) and a slow component (attributed to Ho^{3+} $^5I_6 \rightarrow {}^5I_8$ transition).

Rare earth ion: *4f* electrons shielded by 5s and *5p* electrons ⇒ long lifetime

Si band edge lifetime (blue) is detector speed limited.

Temperature quenching of luminescence

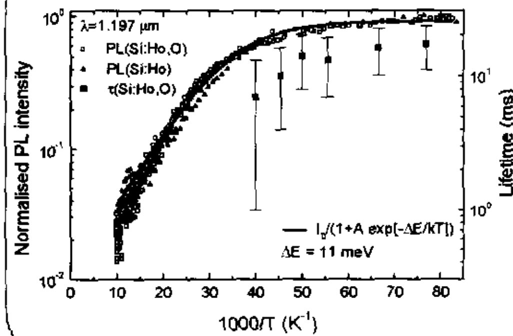

Temperature quenching of luminescence has activation energy of 11 meV.

Carrier concentration

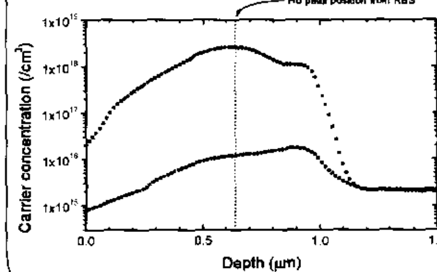

Free carriers may quench luminescence.

Free carrier concentration measured by spreading resistance analysis ⇒

1) Ho is donor in CZ-Si.

2) O co-doping enhances free carrier concentration by two orders of magnitude, ~20% of all Ho is electrically active.

Ho excitation model

Comparable PL quenching behavior with, and without O, while the carrier concentrations in the samples are quite different ⇒
PL quenching is not due to Auger quenching to free carriers.

This leaves only two processes that could be the cause of the observed PL quenching: backtransfer and electron-hole pair dissociation.

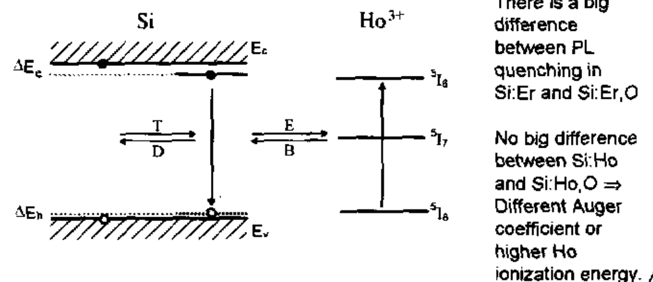

There is a big difference between PL quenching in Si:Er and Si:Er,O

No big difference between Si:Ho and Si:Ho,O ⇒ Different Auger coefficient or higher Ho ionization energy.

Conclusions

- Ho incorporated in Si by ion implantation. Segregation during SPE is suppressed by O co-doping.
- Luminescence observed at λ=1.197, 1.97 and 2.05 μm; attributed to Ho^{3+}.
- Lifetime approximately 14 ms: typical for rare earth luminescence.
- Quenching of the luminescence with an activation energy of 11 meV.
- Data can be described by: backtransfer or electron-hole pair dissociation.